Article

Experimental Study of an Industrial Data Transmission Network in the Automatic Control System of a Wind Turbine

Alina Fazylova [1,2,*], **Baurzhan Tultayev** [2], **Teodor Iliev** [3,*], **Ivaylo Stoyanov** [4], **Mirey Kabasheva** [2] **and Selahattin Kosunalp** [5]

1   Department of Electronics and Robotics, Almaty University of Power Engineering and Telecommunications named after G.Daukeev, Almaty 050013, Kazakhstan

2   Department of Transport Equipment and Organization of Transportation, LB Goncharov Kazakh Automobile and Road Institute, pr. Rayymbeka, 417, Almaty 050061, Kazakhstan; b.tultaev@mail.ru (B.T.); mirey7@yandex.ru (M.K.)

3   Department of Telecommunications, University of Ruse, 8 Studentska Str., 7004 Ruse, Bulgaria

4   Department of Electric Power Engineering, University of Ruse, 8 Studentska Str., 7004 Ruse, Bulgaria; stoyanov@uni-ruse.bg

5   Department of Software Engineering, Bandırma Onyedi Eylül University, Bandırma 10200, Turkey; skosunalp@bandirma.edu.tr

*   Correspondence: a.fazylova@aues.kz (A.F.); tiliev@uni-ruse.bg (T.I.)

Abstract: This article explores and optimizes network technologies for wind energy systems, focusing on the RS-485 interface to ensure reliable data transmission in extreme conditions. The study aims to address the impact of various distortions on data quality and wind turbine management. A system was proposed with two wind turbines, each equipped with a Raspberry Pi 4, connected to sensors measuring temperature, vibration, and wind speed. The research examined how data transmission rates affect signal shape, calculating the distortion coefficient. At 460,800 baud, the signal was almost completely distorted, with significant amplitude loss. The distortion coefficients were 1.84 for logic '1' and 1.92 for logic '0'. The optimal speed to minimize distortions was found to be 19,200 baud, providing the most stable signal. Additionally, temperature significantly impacted transmission quality, highlighting the need to consider climatic conditions in system design. The findings and methods can help improve existing data transmission systems and enhance wind turbine performance.

Keywords: RS-485 interface; data transmission; wind turbine; distortion coefficient; transmission speed

1. Introduction

The modern world is witnessing a significant shift towards renewable energy sources (RES) in an effort to reduce carbon dioxide emissions and mitigate the catastrophic effects of climate change. Among RES, wind energy plays a pioneering role, and its importance is essential for optimizing wind turbine technology [1]. However, despite notable technological advancements in wind turbine design and operation, challenges remain in ensuring reliable data transmission within wind turbine control systems. Wind energy is a more reliable renewable energy resource as it is less affected by environmental factors such as humidity and dust compared to solar energy sources [2]. Wind turbines can be classified into two main categories based on the orientation of their rotating axis: horizontal-axis wind turbines (HAWTs) and vertical-axis wind turbines (VAWTs). HAWTs, being more common, typically require advanced control systems involving pitch and yaw mechanisms to optimize energy capture and alignment with the wind. In contrast, VAWTs, while often less efficient, are simpler in design and operation, relying on more straightforward control systems due to their ability to capture wind from any direction. Ensuring efficient and reliable data transmission for both types of turbines is crucial to maximizing their operational

performance, particularly under varying environmental conditions. The effectiveness of control systems in wind turbines directly depends on the accuracy and timeliness of the data exchanged between components.

Efficient and reliable data exchange is essential for optimizing wind turbine performance and ensuring safety. The RS-485 interface has been widely adopted in industrial automation due to its long-distance communication capabilities and high noise immunity, making it a suitable choice for wind turbine control systems [3]. The rapid growth of wind energy, highlighted by the International Energy Agency as one of the fastest-growing sectors in renewable energy, demands not only an increase in installations but also improvements in operational efficiency. In 2023 alone, global renewable energy capacity grew by 50%, with significant contributions from countries like China, the EU, the USA, and Brazil. To support this expansion, modern policies are focusing on decarbonization and boosting the share of renewable energy sources, as illustrated in Figure 1. Achieving these ambitious goals requires enhancing the reliability and efficiency of wind turbine control systems, particularly in terms of data transmission [4]. To achieve these ambitious goals, it is essential to ensure the reliability and efficiency of wind turbine control systems, particularly in terms of data transmission. Reliable data transmission is especially critical under harsh environmental conditions, such as fluctuating temperatures and electromagnetic interference, where the stability of signals can directly impact the performance and safety of wind turbines.
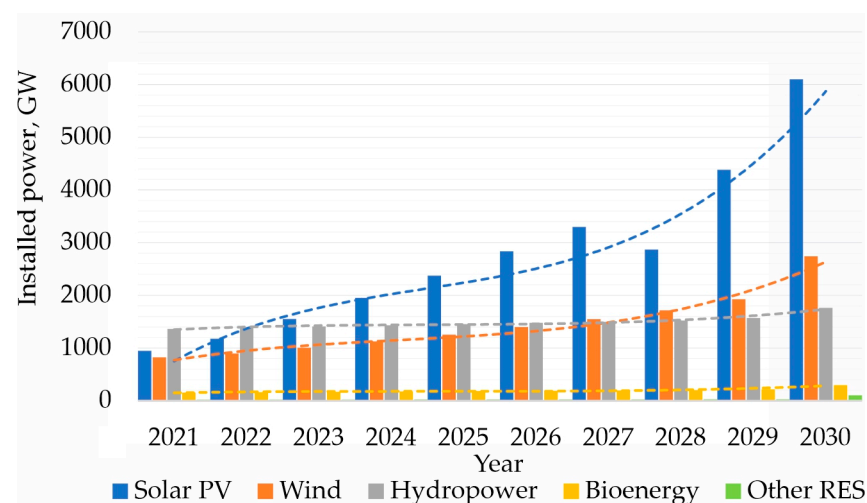
Figure 1. Trends of the cumulative renewable electricity capacity by technologies.

A comparative analysis was conducted to evaluate different data transmission interfaces commonly used in industrial and wind turbine control systems, including RS-232, CAN, Modbus, and Ethernet-based protocols. RS-232, despite its widespread use, has a limited communication distance (up to 15 m) and lower resistance to electromagnetic interference, making it unsuitable for large-scale wind turbine networks [5]. CAN and Modbus provide higher noise immunity and support longer distances but are limited in terms of data rates and the number of devices they can support [6]. Ethernet-based protocols offer high-speed communication and support a large number of devices but are prone to higher transmission delays in harsh conditions, which can be detrimental to real-time wind turbine control [6]. Based on these comparisons, the RS-485 interface was selected as the optimal choice due to its balance of long-distance communication, high noise immunity, and flexibility in multi-point networks [7].

This study addresses these challenges by focusing on the use of the RS-485 interface for data transmission in wind turbine control systems. The RS-485 interface, known for its high noise immunity and long-distance communication capabilities, was analyzed under different transmission speeds and environmental conditions to evaluate its performance in complex operational scenarios. The primary contribution of this work is the development of

an experimental setup and a mathematical model to analyze signal distortions, transmission delays, and the impact of temperature variations on data quality.

The primary task in wind turbine management is to ensure the maximum efficiency of their operation, which directly depends on the accuracy and timeliness of the operational data received. Data on wind speed, blade loads, temperature, and other critical parameters must be transmitted in real-time with minimal delays and distortions [8–10]. However, in practice, data transmission networks often encounter problems caused by external interference, physical obstacles, and equipment limitations [11]. This makes it critically important to study and optimize network technologies in the context of wind energy installations. RS-485 expresses the characteristics for drivers and receivers in balanced digital multipoint systems, making it ideal for environments requiring long-distance communication and high noise immunity [12]. It uses differential signalling, allowing for data transmission over distances up to 1200 m and supporting up to 32 devices on a single bus [13]. The differential voltage ranges from −7 V to +12 V, with termination resistors at both ends to prevent reflections and biasing resistors to maintain a stable state [14].

RS-485 operates in half-duplex or full-duplex modes and is widely used in industrial automation, building automation, instrumentation, data acquisition, access control systems, solar power systems, and medical equipment due to its robustness and noise immunity [15].

Modern wind energy management systems require highly reliable data transmission to ensure efficient operation under varying external influences. A key element of such systems is the resilience of data transmission against external interference and the ability to adapt to changing operating conditions. However, most existing solutions do not simultaneously consider the impact of transmission speed and environmental factors such as temperature fluctuations and interference. This gap necessitates further investigation into network parameters and the adaptation of transmitting devices to improve signal quality [16].

In this study, a comprehensive approach is proposed that involves the mathematical modelling and analysis of data transmission characteristics using the RS-485 interface. The RS-485 interface, known for its high noise immunity and long-distance communication capabilities, was analyzed under different transmission speeds and environmental conditions to evaluate its performance in complex operational scenarios [16]. The novelty of the work is as follows:

A method for evaluating signal distortions and transmission delays under varying environmental parameters and at different data transmission speeds has been developed.

An optimal transmission mode has been proposed to ensure minimal signal distortion, which enhances communication reliability in industrial conditions.

For the first time, the influence of temperature on the signal distortion coefficient is examined in detail, allowing recommendations to be made for selecting transmission parameters in fluctuating environmental conditions.

The advantage of the proposed approach lies in its ability to consider the full spectrum of possible network parameter changes, providing a comprehensive assessment of data transmission resilience and offering recommendations to improve the efficiency of wind turbine control systems. This makes the results of the study a valuable contribution to the development of reliable data transmission technologies in the energy sector.

2. Materials and Methods

2.1. Model of a Vertical-Axis Wind Turbine

The wind turbine used in this study is a Darrieus-type vertical-axis wind turbine (VAWT), a configuration known for its simplicity and suitability for various environments, particularly urban areas. This turbine is designed with three straight blades positioned symmetrically around a central axis, allowing it to capture wind from any direction without the need for complex yaw or pitch mechanisms, which are typically found in horizontal-axis wind turbines (HAWTs) [17]. The chosen turbine model operates at wind speeds ranging from 3 m/s to 12 m/s, with a cut-in speed of 3 m/s and an optimal performance at wind speeds around 8 m/s. This makes the Darrieus turbine versatile and capable of

functioning in environments with moderate and variable wind conditions. The turbine's power coefficient (Cp), which measures its efficiency in converting wind energy into mechanical power, typically ranges from 0.35 to 0.45. These features align with the study's goal of optimizing the RS-485 data transmission system for efficient wind turbine control under varying environmental conditions [18].

The Darrieus VAWT model shown in Figure 2 was developed in SolidWorks and highlights the turbine's geometric and mechanical characteristics. This model is essential for evaluating how the data transmission system performs when integrated with wind turbine control systems, ensuring the reliable communication of critical parameters such as wind speed, blade loads, and temperature. The robustness of the RS-485 interface in handling environmental factors like electromagnetic interference, vibrations, and temperature fluctuations is key to the study's objective of enhancing the reliability of wind turbine control systems. By analyzing this turbine design, the research demonstrates how optimized data transmission contributes to the operational efficiency and safety of wind turbines, particularly in challenging environmental conditions.
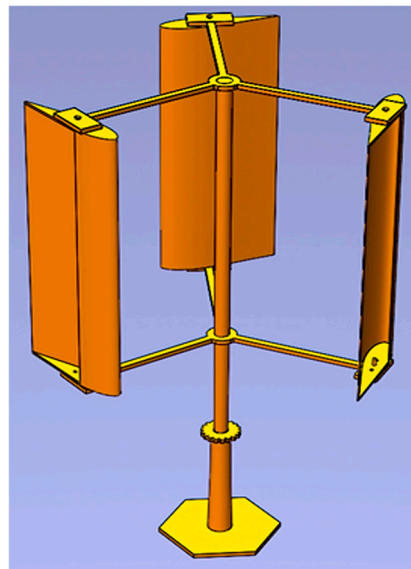
Figure 2. SolidWorks Model of the Darrieus Vertical-Axis Wind Turbine (VAWT).

The wind turbine operates at varying wind speeds throughout the year, and changes in wind speed can potentially influence the efficiency of data transmission systems. The average hourly wind speed over the year is around 5.8 mph [19]. Table 1 shows the monthly average wind speeds [20]. The wind speed varies between 5.4 mph in January and 6.2 mph in May, illustrating a relatively stable wind environment with moderate fluctuations. The cut-in speed of the turbine, approximately 3 m/s (6.7 mph), is met consistently during the year, ensuring regular turbine operation. This data provides insight into how the wind speed in the turbine's environment fluctuates over the year. The average wind speed is consistently above the turbine's cut-in speed, ensuring regular energy production and a steady flow of operational data. These operating conditions are critical for assessing the performance of the RS-485 data transmission system in maintaining reliable communication under real-world environmental fluctuations. The wind speed peaks around 6.2 mph in May and averages around 5.4 to 6.1 mph throughout the rest of the year, providing consistent operational conditions for the wind turbine and its data transmission system.

Table 1. Average wind speed in Almaty by month.

| Month	Feb	Mar	Apr	May	Jun	Jul	Aug	Sep	Oct	Nov	Dec	Feb
Wind Speed (mph)	5.4	5.5	5.8	6.2	6.1	6.0	6.1	6.0	5.9	5.6	5.5	5.4

2.2. Data Collection Network

A very important task is reliable data transmission systems that can function in extreme conditions and maintain high levels of wind turbine performance [21]. This research aims to study and optimize network technologies in the context of wind energy installations, focusing on the RS-485 interface to develop robust and reliable data transmission systems. The relevance of this research is supported by the need to address the impact of various types of distortions on data transmission quality and subsequent wind turbine management [22,23]. The study involves theoretical analysis and practical testing to identify optimal parameters for minimizing delays and errors, contributing to the improvement of designs and control algorithms and increasing the overall reliability and economic efficiency of wind energy projects [24–26].

The system consists of a central control unit and two wind turbines. This network represents a data collection system from two wind turbines, each equipped with a Raspberry Pi 4 Model B, Cambridge, UK connected to temperature sensors (DHT22), vibration sensors, and wind speed sensors (anemometers) [27]. Data from the sensors are transmitted through USB3.0adapters to an RS-485 switch, which consolidates the data and sends them to a central server, also based on a Raspberry Pi 4 Model B, Cambridge, UK connected via a similar adapter. The server, connected to the internet, processes and transmits the collected data for remote monitoring and system management (Figure 3).

To describe the data transmission process between the wind turbines and the central control unit, a signal transmission model using the RS485 (EIA/TIA-485) [27] interface is employed [28]. It is among the most commonly adopted physical layer standards in contemporary industrial automation. This standard details the electrical attributes of receivers and transmitters capable of binary signal transmission in multipoint networks. Nevertheless, it does not address other factors such as signal quality, communication protocols, connector types, or transmission lines.

This omission often leads to difficulties for users when connecting different devices to an RS-485 network. An inadequately designed RS-485 network can undermine automation efforts, causing frequent equipment failures, malfunctions, and errors [29]. The aim of this article is to offer users recommendations for connecting and practically implementing data transmission systems using the RS-485 interface [30]. The RS-485 interface employs differential (balanced) data transmission. This technique involves transmitting a normal signal on one wire (referred to as line A) and an inverted signal on another wire (referred to as line B), ensuring a constant potential difference between the two wires of the twisted pair (Figure 3). For a logical "one", the potential difference is positive, while for a logical "zero", it is negative [31].

The advantage of differential (balanced) data transmission is its high resistance to common-mode noise, which affects both communication lines equally. In areas with non-uniform electromagnetic fields, an electromagnetic wave induces a potential in both wires. Unlike RS-232, where the useful signal relative to the "ground" could be lost, differential transmission maintains the signal's integrity by keeping the potential difference (useful signal) unchanged. RS-485 uses twisted pair wires, with direct outputs "A" connected to one wire and inverted outputs "B" to the other. Incorrect connections will not damage the transceivers but will prevent proper function. It is worth mentioning that to maintain reliability and reduce noise interference, it is advisable to decrease the data transmission speed as the length of the communication lines increases.
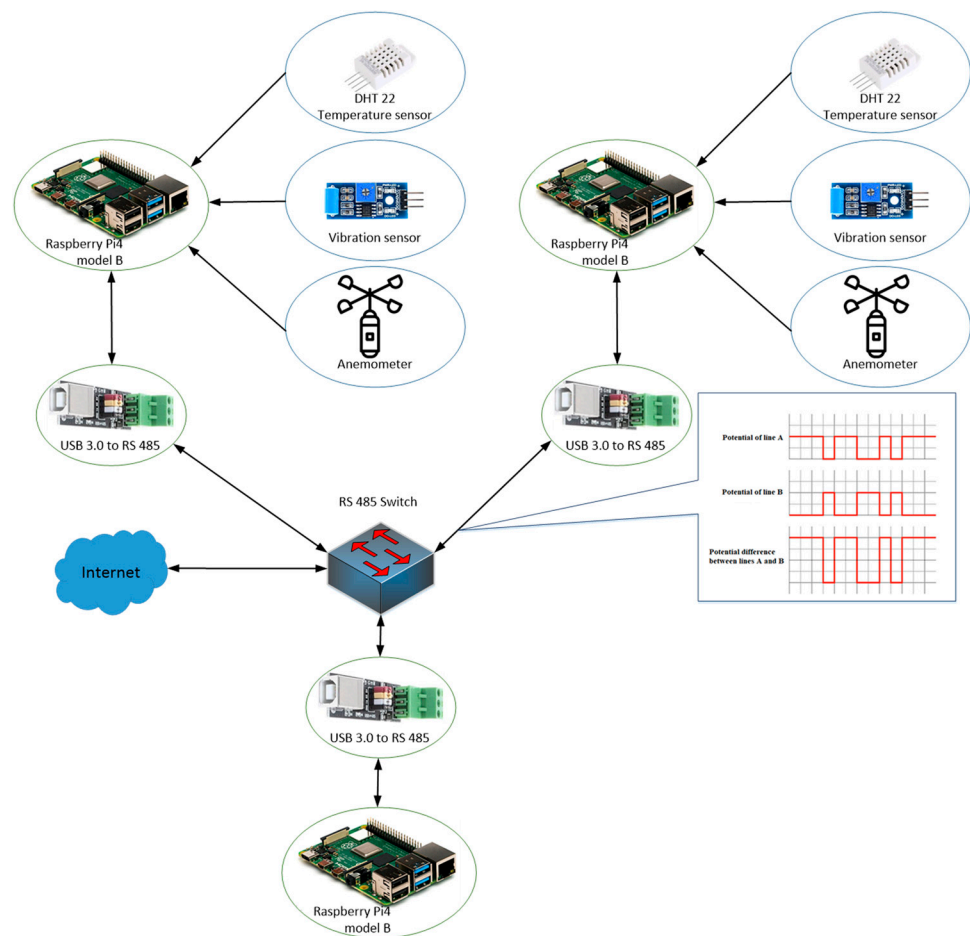
Figure 3. Data collection network from wind turbines based on Raspberry Pi and RS-485 interface.

The signal transmitted through the RS-485 interface can be described as a sinusoidal signal with additive noise. The mathematical model of the signal is as follows [32]:

$$V(t) = A sin(2\pi f t + \varphi) + N(t),$$ (1)

where the amplitude of the signal is denoted with A, the frequency is f and φ is the phase of the signal, and N is the additive noise.

The transmission of the signal through the channel can be described by the convolution equation [3]:

$$V_{out}(t) = \int_{-\infty}^{\infty} v_{in}(\tau)h(t-\tau)\mathrm{d}\tau + N(t),$$ (2)

where with $h(t)$ is denoted the impulse response of the channel.

$h(t)$ describes how the signal changes as it passes through the data transmission channel. For our case, let us assume that the channel has an exponential impulse response [33]:

$$h(t) = \mathrm{e}^{-\alpha t}$$ (3)

Let us substitute the signal and the impulse response into the convolution equation:

$$V_{out}(t) = A \int_{-\infty}^{\infty} sin(2\pi f \tau + \varphi)\mathrm{e}^{-\alpha(t-\tau)}\mathrm{d}\tau + \int_{-\infty}^{\infty} N(\tau)\mathrm{e}^{-\alpha(t-\tau)}\mathrm{d}\tau + N(t)$$ (4)

To evaluate signal distortions, the distortion coefficient *K* is used, which is defined as the ratio of the signal energy at the input to the signal energy at the output [34]:

$$k = \frac{\int |V_{in}(t)|^2 \mathrm{d}t}{\int |V_{out}(t)|^2 \mathrm{d}t} \tag{5}$$

To determine the signal delay time in the system, correlation analysis is used [35]:

$$\tau_{max} = argmax_\tau (\int V_{in}(t)V_{out}(t+\tau)dt), \tag{6}$$

where τ_{max} is the time delay with maximum correlation between input and output signals.

Next, the method of integration by parts and properties of sinusoidal functions were used:

The energy of the input and output signals can be calculated using the following formulas [36]:

$$V_0(t) = Asin(2\pi ft + \varphi) \cdot \frac{1}{\sqrt{\alpha^2 + (2\pi f)^2}} \tag{7}$$

$$E_{in} = \int_0^T \mathrm{A}(sin(2\pi ft + \varphi))^2 \mathrm{d}t = \frac{A^2 T}{2} \tag{8}$$

$$E_{out} = \int_0^T \mathrm{A}(sin(2\pi ft + \varphi)) \frac{1}{\sqrt{\alpha^2 + (2\pi f)^2}} \mathrm{d}t = \frac{A^2 T}{2(\alpha^2 + (2\pi f)^2)} \tag{9}$$

Hence, it follows that the distortion coefficient is equal to:

$$k = \frac{E_{in}}{E_{out}} = \alpha^2 + (2\pi f)^2 \tag{10}$$

The correlation function for the delay [37]:

$$R_{v_{in}, v_{out}}(\tau) = \int_0^T V_{in}(t)V_{out}(t+\tau)\mathrm{d}t \tag{11}$$

The maximum correlation is achieved when:

$$\tau_{max} = \frac{1}{2\pi f} \tag{12}$$

In addition to the theoretical model described earlier, a real-world implementation of the system was constructed to test data transmission performance in practical conditions. This network consists of two wind turbines, each equipped with a Raspberry Pi 4 Model B connected to various sensors, such as temperature sensors (DHT22), vibration sensors, and wind speed sensors. The Raspberry Pi devices are connected via USB3.0-RS-485 adapters, which transmit the data to an RS-485 switch. This switch sends the data to a central server, also based on a Raspberry Pi 4 Model B, connected via a similar RS-485 adapter. The entire system is connected to a modem for real-time data transmission and remote monitoring [38]. Additionally, a weather station with an anemometer is installed on the roof, transmitting data wirelessly to the central system. The complete system layout is illustrated in Figure 4, showing the hardware connections and system components. This physical implementation allows for monitoring the data transmission performance and validating the mathematical model presented in the study.
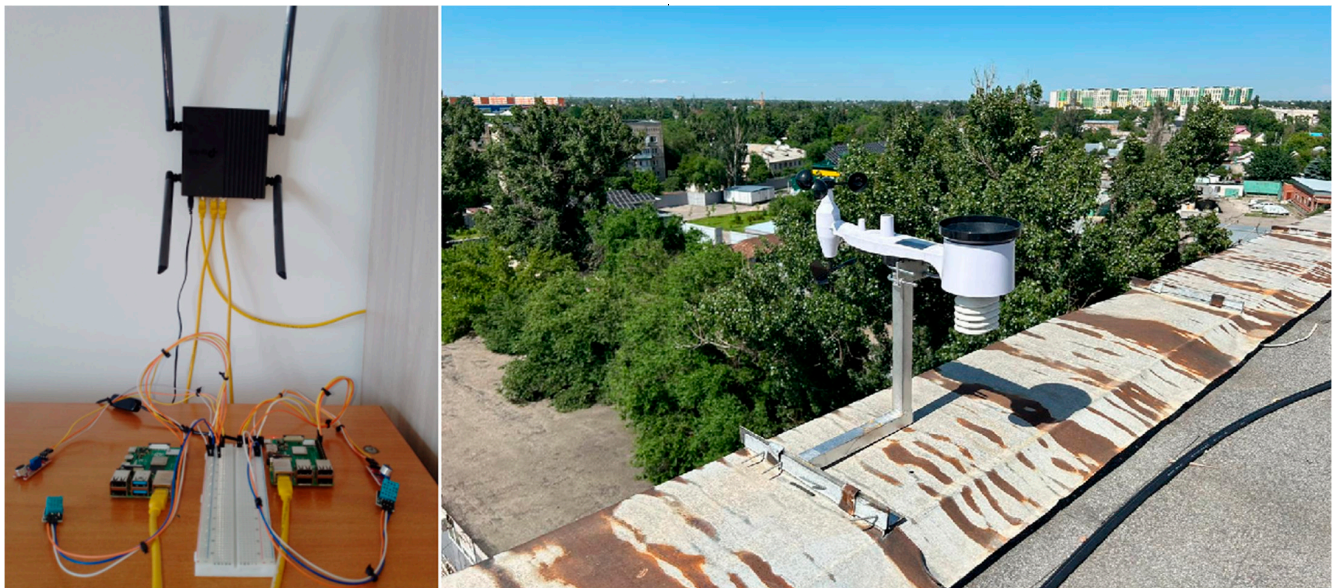
Figure 4. Hardware Layout of the Wind Turbine Monitoring System Based on Raspberry Pi and RS-485 Interface.

To ensure reliable data transmission in wind turbine control systems, it is important to consider various environmental factors that can influence signal quality. These factors include electromagnetic interference, mechanical vibrations, long communication distances, and temperature variations. Electromagnetic interference is typically caused by high-power electronics and electrical components within the turbine, while mechanical vibrations are induced by the continuous movement of the blades and nacelle.

Additionally, temperature fluctuations can alter the signal properties, potentially increasing the distortion coefficient and affecting the stability of data transmission. The influence of temperature can potentially alter the distortion coefficient, impacting the stability and reliability of the RS-485 interface in real-world scenarios.

3. Results and Discussion

During transmission through real communication channels, signals undergo distortions, resulting in received messages being reproduced with some errors. The errors are caused by interfering signals, changes in transmission line impedance, and environmental factors such as temperature and mechanical effects. These factors can lead to signal degradation, increased delays, and data transmission errors. The experimental setup utilized a 300 m RS-485 communication line, which, while shorter than the maximum recommended length of 1200 m for RS-485, was chosen to simulate typical industrial conditions. This length ensured that the results accurately reflect real-world performance while maintaining a stable communication link between devices. Figures 5–18 show the signal waveforms at different data transmission rates, ranging from 4800 to 460,800 baud, measured at the input of the network and at the input of the nearest and furthest slave device.

The experimental setup included several slave devices positioned along the communication line, with the furthest device placed at the end of the 300 m cable. This configuration was designed to evaluate signal integrity and transmission quality over a realistic distance for industrial applications. The selected cable length ensured the system could simulate typical communication scenarios encountered in wind turbine networks, where long-distance data transmission is necessary. The results showed that data rates up to 19,200 baud provided stable transmission with minimal distortion, while higher data rates led to noticeable signal degradation. The choice of a 300 m line length reflects practical considerations and the need to test the reliability of the RS-485 interface under realistic operating conditions.
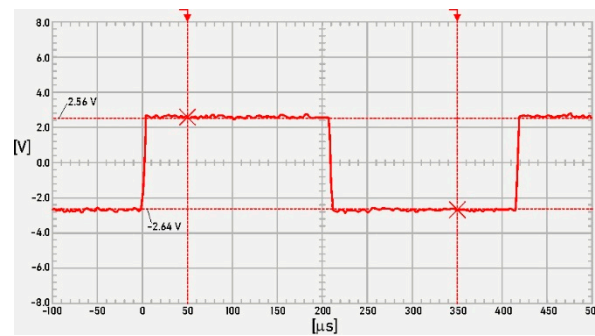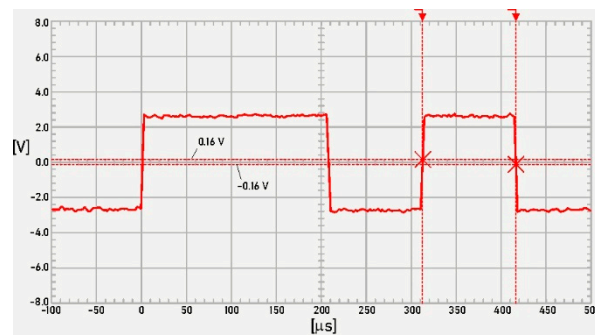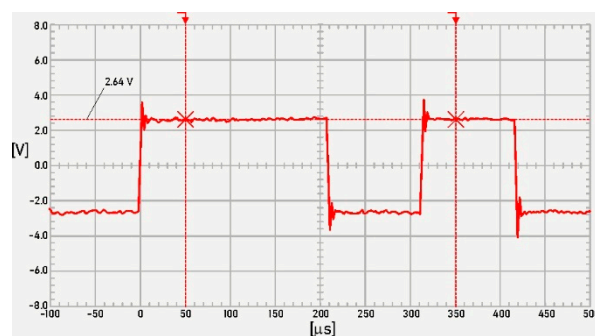
Figure 5. The signal waveform at the input of the network at a speed of 4800 baud (dX = 300 ms, dY = 5.20 V).The markers (×) show the cross point between the signal and the markers.
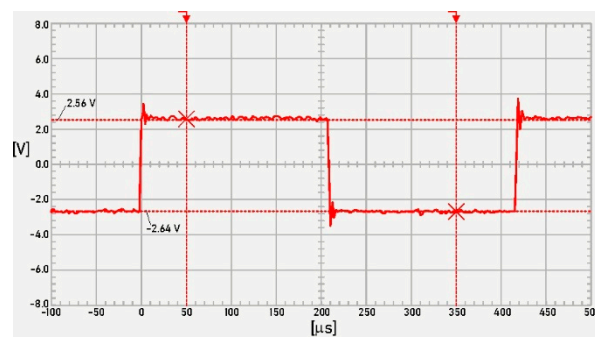
Figure 6. The signal waveform at the input of the slave device at a speed of 4800 baud (dX = 300 ms, dY = 5.20 V). The markers (×) show the cross point between the signal and the markers.
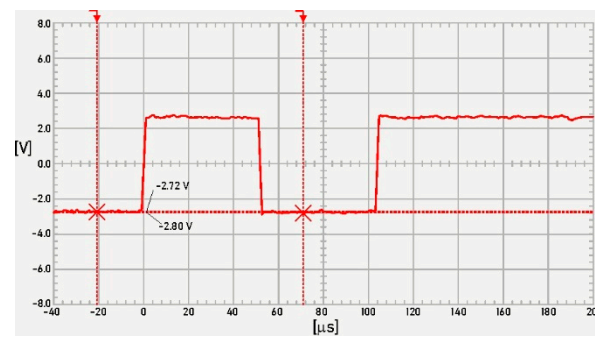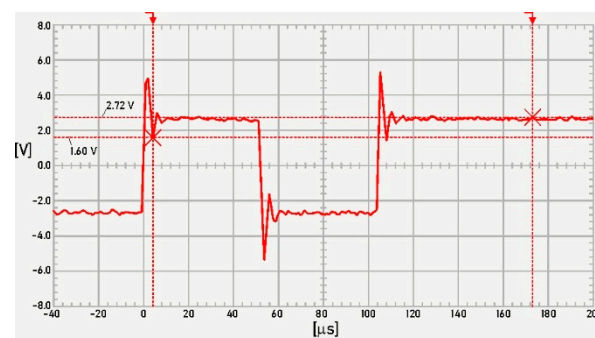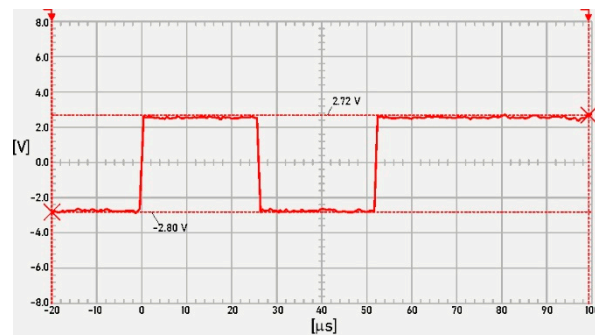

Figure 7. The signal waveform at the input of the network at a speed of 9600 baud (dX = 300 ms, dY = −0.32 V). The markers (×) show the cross point between the signal and the markers.

Figure 8. The signal waveform at the input of the slave device at a speed of 9600 baud (dX = 300 ms, dY = 0 V). The markers (×) show the cross point between the signal and the markers.

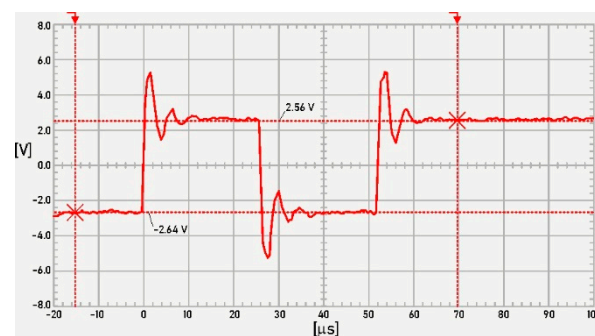**Figure 9.** The signal waveform at the input of the network at a speed of 19,200 baud (dX = 300 ms, dY = 0.08 V). The markers (×) show the cross point between the signal and the markers.
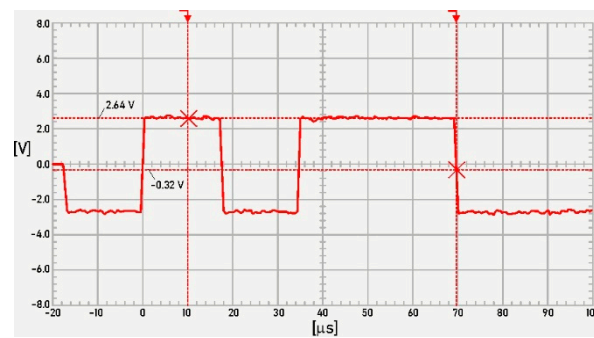

Figure 10. The signal waveform at the input of the slave device at a speed of 19,200 baud (dX = 300 ms, dY = 1.12 V). The markers (×) show the cross point between the signal and the markers.
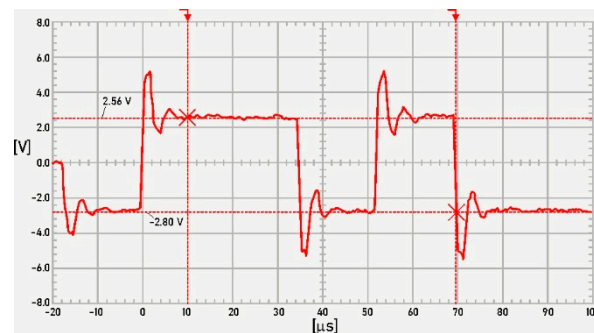

Figure 11. The signal waveform at the input of the network at a speed of 38,400 baud (dX = 300 ms, dY = 5.52 V). The markers (×) show the cross point between the signal and the markers.
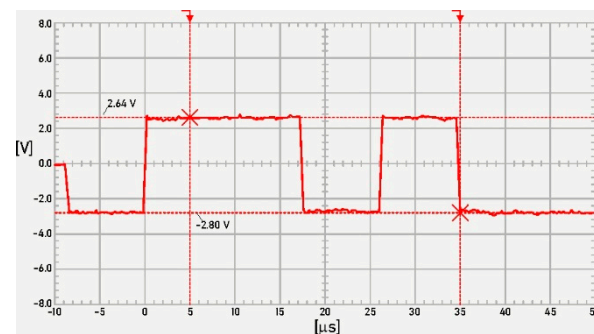

Figure 12. The signal waveform at the input of the slave device at a speed of 38,400 baud (dX = 300 ms, dY = 5.20 V). The markers (×) show the cross point between the signal and the markers.

Figure 13. The signal waveform at the input of the network at a speed of 57,600 baud (dX = 300 ms, dY = −2.96 V). The markers (×) show the cross point between the signal and the markers.

Figure 14. The signal waveform at the input of the slave device at a speed of 57,600 baud (dX = 300 ms, dY = 5.36 V). The markers (×) show the cross point between the signal and the markers.
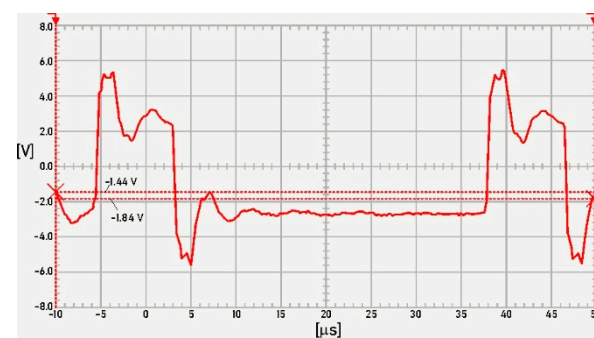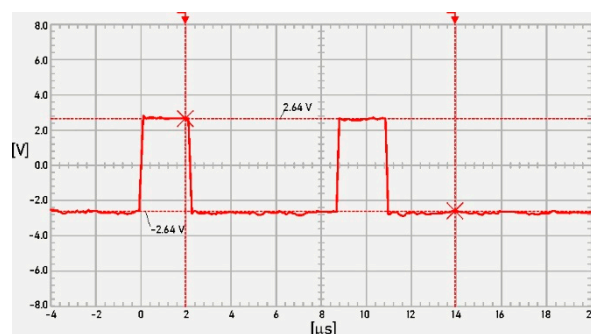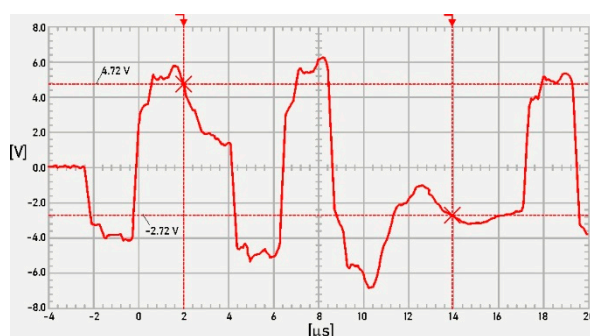

Figure 15. The signal waveform at the input of the network at a speed of 115,200 baud (dX = 300 ms, dY = 5.44 V). The markers (×) show the cross point between the signal and the markers.

Figure 16. The signal waveform at the input of the slave device at a speed of 115,200 baud (dX = 300 ms, dY = −0.40 V). The markers (×) show the cross point between the signal and the markers.

Figure 17. The signal waveform at the input of the network at a speed of 460,800 baud (dX = 300 ms, dY = −5.28 V). The markers (×) show the cross point between the signal and the markers.

Figure 18. The signal waveform at the input of the slave device at a speed of 460,800 baud (dX = 300 ms, dY = −7.44 V). The markers (×) show the cross point between the signal and the markers.

The RS-485 interface employs a differential (balanced) method of data transmission. In this method, the potential difference at the output of the transceiver changes: for transmitting '1', the potential difference between A and B is positive, and for transmitting '0', the potential difference between A and B is negative. To accurately capture the signal characteristics at both the generator and slave device nodes, differential probes were used, ensuring that common-mode noise was minimized and the true signal values were recorded. This setup ensured the accurate measurement of the differential signal and minimized the influence of interference, typical for industrial environments.

The waveforms at the network input and the slave device input at various data transmission speeds are shown in Figures 5–18, where dX, dY—steps along the time and voltage axes, respectively. These graphs demonstrate how the signal shape changes depending on the transmission speed.

At a speed of 4800 baud, the signal shape at the network input is practically undistorted, while at the slave device input, there is a slight decrease in signal amplitude, but the signal shape remains clear and distinct. The distortion coefficient for logic '1' is approximately 1.04, and for logic '0' it is about 0.98.

At 9600 baud, the signal shape at the network input remains almost unchanged compared to 4800 baud, and at the slave device input, the signal amplitude also slightly decreases, but the shape remains clear. The distortion coefficient for logic '1' is approximately 1.05, and for logic '0' it is about 0.97.

At 19,200 baud, the signal at the network input remains almost unchanged, and the signal shape is well distinguishable. There is a slight increase in distortion at the slave device input, but the signal shape remains distinguishable. The distortion coefficient for logic '1' is approximately 1.05, and for logic '0' it is about 0.99.

At 38,400 baud, the signal shape at the network input starts to distort slightly, and the signal amplitude decreases. At the slave device input, there is a significant decrease in

signal amplitude, and the signal shape begins to distort. The distortion coefficient for logic '1' is approximately 1.09, and for logic '0' it is about 1.02.

At 57,600 baud, the signal shape at the network input becomes less clear, and the signal amplitude noticeably decreases. At the slave device input, the signal is significantly distorted, and the signal amplitude decreases significantly. The distortion coefficient for logic '1' is approximately 1.09, and for logic '0' it is about 1.05.

At 115,200 baud, the signal shape at the network input is heavily distorted, and the signal amplitude decreases significantly. At the slave device input, the signal is heavily distorted, and the signal amplitude decreases substantially. The distortion coefficient for logic '1' is approximately 1.19, and for logic '0' it is about 1.11.

At 460,800 baud, the signal at the network input is almost completely distorted, and the signal amplitude decreases significantly. At the slave device input, the signal is completely distorted, and the signal amplitude is minimal. The distortion coefficient for logic '1' is approximately 1.84, and for logic '0' it is about 1.92.

Thus, the optimal data transmission speed for minimizing distortions is in the range up to 19,200 baud. At these speeds, the signal shape is most stable and less susceptible to distortion. With increasing data transmission speeds, distortions increase, indicating a deterioration in data transmission quality at higher speeds. This may be due to physical limitations of the equipment and increased noise and interference. The distortion coefficient of the signal was calculated using the formula:

$$K_i = \frac{S_{in}}{S_{out}}, \tag{13}$$

where S_{in}—the area under the signal waveform at the input of the slave device; S_{out}—the area under the signal waveform at the output of the generator.

The approximate area under the signal waveform was calculated using the formula:

$$S \approx \sum_{i}^{n-1} U_i \Delta t, \tag{14}$$

where U_i the voltage value of the signal at point i; Δt time interval.

The results of the experiments are presented in Table 2, showing the distortion coefficient of the signal waveform.

Table 2. Signal distortion at different data transmission speeds.

Speed	Distortion Coefficient	
	K_i **(Logic 1)**	K_i **(Logic 0)**
4800	1.04	0.98
9600	1.05	0.97
19,200	1.05	0.99
38,400	1.09	1.02
57,600	1.09	1.05
115,200	1.19	1.11
460,800	1.84	1.92

Further, a Python code was developed to compute the relationship between the distortion coefficient and the data transmission speed (Figure 19). The code for correlation analysis is shown on Figure 20.

```
import numpy as np
import matplotlib.pyplot as plt
speeds = np.array([4800, 9600, 19200, 38400, 57600, 115200, 460800])
distortion_1 = np.array([1.04, 1.05, 1.05, 1.09, 1.09, 1.19, 1.84])
distortion_0 = np.array([0.98, 0.97, 0.99, 1.02, 1.05, 1.11, 1.92])
plt.figure(figsize=(10, 6))
plt.plot(speeds, distortion_1, label="Ki when logic 1", marker='o')
plt.plot(speeds, distortion_0, label="Ki when logic 0", marker='s')
plt.xlabel("Data transmission speed (baud)")
plt.ylabel("Distortion coefficient ")
plt.title("Distortion coefficient at different data transmission speeds ")
plt.legend()
plt.grid(True)
plt.show()
```

Figure 19. Python code for the computation of the relationship between the distortion coefficient and the data transmission speed.

```
# Data for signal frequency
frequencies = np.array([50, 100, 200, 400, 800, 1600, 3200])
#Calculation of time delay
delay_times = 1 / (2 * np.pi * frequencies)
# Plotting the signal delay graph
plt.figure(figsize=(10, 6))
plt.plot(frequencies, delay_times, label=" Signal delay time ", marker='o')
plt.xlabel("Signal frequency (Hz)")
plt.ylabel("Time delay (seconds)")
plt.title("The dependence of the delay time on the signal frequency ")
plt.legend()
plt.grid(True)
plt.show()
```

Figure 20. Python code for the correlation.

This code facilitated the generation of the graphs in Figures 21 and 22, which depict the calculated distortion coefficient and signal delay times for different transmission speeds. The algorithm uses temperature and transmission speed inputs to model and visualize how these variables affect signal quality and delay, providing essential insights for optimizing the system's performance under varying environmental conditions. As a result, the graphs shown in Figures 21 and 22 were obtained.
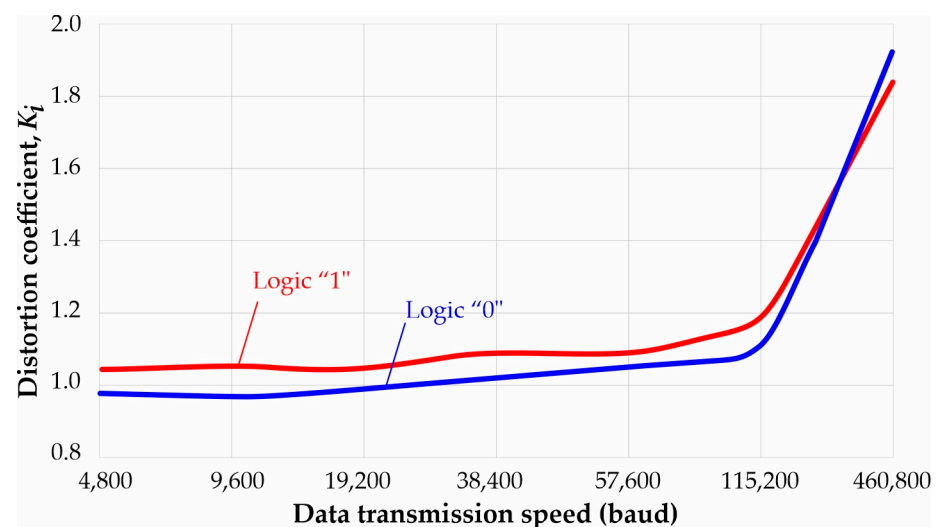
Figure 21. Distortion coefficient at different data transmission speeds.
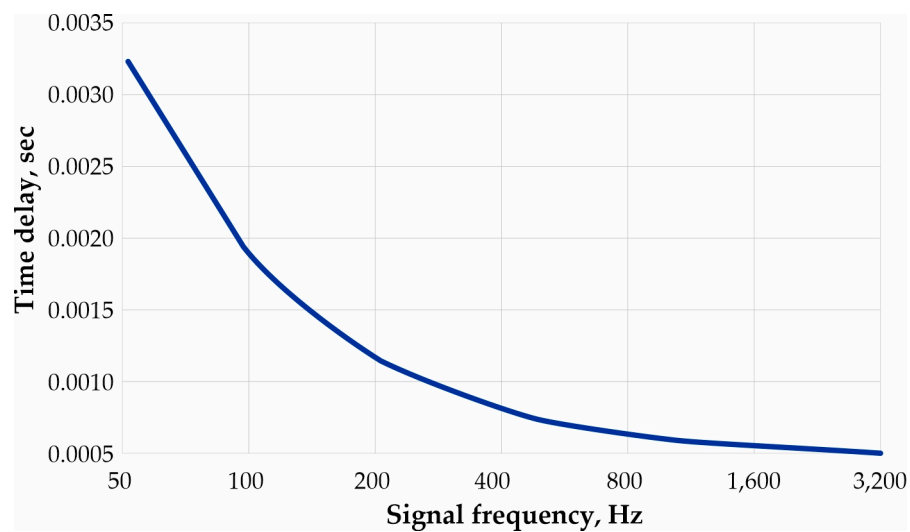
Figure 22. The dependence of delay time on signal frequency.

From Figure 21, it can be observed that at low data transmission speeds (4800 baud), the distortion coefficient K_i remains around 1.04 for logic '1' and 0.98 for logic '0'. As the data transmission speed increases to 19,200 baud, the distortion coefficients remain practically unchanged, staying within 1.05 and 0.99 respectively. With a further increase in data transmission speed, the distortion coefficient starts to rise. At speeds of 115,200 baud and above, a significant increase in the distortion coefficient is observed, especially for logic '1' (up to 1.84 at 460,800 baud).

Thus, the optimal data transmission speed for minimal signal distortion lies in the range up to 19,200 baud. At these speeds, the signal waveform is most stable and less susceptible to distortion. With increasing data transmission speed, distortions increase, indicating a deterioration in data transmission quality at higher speeds. This may be due to physical limitations of the equipment and increased influence of noise and interference.

Figure 22 demonstrates that the signal delay time is inversely proportional to the signal frequency. This is evident from the decreasing curve, where an increase in signal frequency leads to a decrease in delay time. At low frequencies (50 Hz), the signal delay time is significantly higher (around 3.18 milliseconds). With an increase in frequency to 3200 Hz, the signal delay time decreases to less than 50 microseconds.

Thus, higher signal frequencies result in shorter delays, which can be beneficial for systems requiring rapid response and minimal delays. The choice of signal frequency should balance between data transmission speed requirements and acceptable delays. For systems with critically important time parameters, higher frequencies are preferred. The influence of temperature on the distortion coefficient was also studied using a second-order polynomial model [39]:

$$K_i(t) = K_{i0} \cdot \left(1 + \beta_1(T - T_0) + \beta_2\left(T - T_0\right)^2\right), \tag{15}$$

where K_{i0}—the distortion coefficient at the baseline temperature T_0; β_1—the coefficient of linear temperature influence; β_2—the coefficient of quadratic temperature influence; T—the current temperature.

Initial conditions: Baseline temperature $T_0 = 20\ °C$, the distortion coefficient at the baseline temperature $K_{i0} = 1.05$ (Based on the experiment conducted earlier), the coefficient of linear temperature influence $\beta_1 = 0.01$. The coefficient of quadratic temperature influence $\beta_2 = 0.001$ [40].

The difference between the current temperature and the baseline temperature can be calculated by [40]:

$$\Delta T = T - T_0 \tag{16}$$

The linear contribution was calculated using the formula:

$$\beta_1 \cdot \Delta T \tag{17}$$

The quadratic contribution was also calculated:

$$\beta_2 \cdot (\Delta T)^2 \tag{18}$$

Summing up the contributions will give:

$$1 + \beta_1 \cdot \Delta T + \beta_2 \cdot (\Delta T)^2 \tag{19}$$

Thus, the overall expression obtained is:

$$K_i(t) = K_{i0} \cdot (1 + \beta_1 \Delta T + \beta_2 (\Delta T)^2) \tag{20}$$

For various temperatures, the distortion coefficient was calculated using the methodology described above. The calculation results are recorded in Table 3, where $T_0 = 20\,°C$.

Table 3. Calculation results for Distortion coefficient $K_i(t)$.

T (°C)	$\Delta T = T - T_0$ (°C)	$\beta_1 \cdot \Delta T$	$\beta_2 \cdot (\Delta T)^2$	$1 + \beta_1 \cdot \Delta T + \beta_2 \cdot (\Delta T)^2$	$K_i(t)$
10	−10	0.1	0.1	1	1.05
20	0	0	0	1	1.05
30	10	0.1	0.1	1.2	1.26
40	20	0.2	0.4	1.6	1.68
50	20	0.3	0.9	2.2	2.31

The calculations demonstrate how the distortion coefficient K_i changes with temperature (T), using a second-order polynomial model. This model allows for a more accurate consideration of temperature's influence on signal distortion in data transmission systems.

The inclusion of both linear (β_1) and quadratic (β_2) temperature terms allows for a detailed representation of how temperature deviations from the baseline of 20 °C affect the transmission quality. As temperature increases or decreases, the distortion coefficient also increases, indicating greater instability at extreme temperatures, such as 50 °C. These results offer valuable insights for optimizing data transmission systems under a wide range of operational temperature conditions, ensuring the system's resilience and stability in varying climates. By understanding the effects of temperature, engineers can adjust transmission parameters to mitigate distortion and improve the overall reliability of wind turbine control systems.

4. Conclusions

The conducted study has demonstrated the importance of optimizing data transmission technologies in wind turbine control systems. In particular, the effectiveness of using the RS-485 interface for data transmission in industrial environments characterized by high levels of electromagnetic interference and physical constraints was examined. The key findings of the study are summarized below:

- Optimal transmission rate: Experimental results showed that a data transmission rate of up to 19,200 baud ensures minimal signal distortion and high transmission stability, making it optimal for these conditions.
- Impact of transmission speed: As transmission speed increases, the distortion coefficient rises, leading to a deterioration in data transmission quality and an increased susceptibility to external influences.

- Climatic considerations: Temperature was found to significantly impact transmission quality, underscoring the need to consider climatic conditions during the design and operation of such systems.

These findings highlight the importance of choosing appropriate data transmission rates and accounting for environmental factors to ensure reliable wind turbine control. The methods developed in this study can be applied to improve existing data transmission systems and to develop new systems, enhancing the reliability and efficiency of wind turbine management across a range of turbine types and sizes, including both vertical-axis and horizontal-axis turbines. This flexibility makes the system suitable for turbines in diverse operational conditions, ensuring robust and efficient data management.

Future research will focus on integrating more advanced technologies and transmission protocols, as well as developing strategies to further minimize the impact of external environmental factors, such as electromagnetic interference and temperature fluctuations, in order to increase the resilience of wind turbine control systems.

Abbreviations

RES	Renewable Energy Sources
HAWTs	Horizontal-Axis Wind Turbines
VAWTs	Vertical-Axis Wind Turbines
VAWT	Vertical-Axis Wind Turbine
DHT22	Type of the temperature sensor

References

1. Ghafoorian, F.; Mirmotahari, S.R.; Wan, H. Numerical study on aerodynamic performance improvement and efficiency enhancement of the savonius vertical axis wind turbine with semi-directional airfoil guide vane. *Ocean. Eng.* **2024**, *307*, 118186. [CrossRef]
2. Ghafoorian, F.; Mirmotahari, S.R.; Mehrpooya, M.; Akhlaghi, M. Aerodynamic performance and efficiency enhancement of a Savonius vertical axis wind turbine with Semi-Directional Curved Guide Vane, using CFD and optimization method. *J. Braz. Soc. Mech. Sci. Eng.* **2024**, *46*, 443. [CrossRef]
3. Ahmed, M.A.; Kim, Y.-C. Communication Network Architectures for Smart-Wind Power Farms. *Energies* **2014**, *7*, 3900–3921. [CrossRef]
4. Holechek, J.L.; Geli, H.M.E.; Sawalhah, M.N.; Valdez, R. A Global Assessment: Can Renewable Energy Replace Fossil Fuels by 2050? *Sustainability* **2022**, *14*, 4792. [CrossRef]
5. Xu, C.; Du, X.; Li, X.; Tu, Y.; Li, L.; Jin, X.; Xia, C. 5G-Based Industrial Wireless Controller: Protocol Adaptation, Prototype Development, and Experimental Evaluation. *Actuators* **2023**, *12*, 49. [CrossRef]
6. Bożek, A.; Rzonca, D. Communication Time Optimization of Register-Based Data Transfer. *Electronics* **2023**, *12*, 4917. [CrossRef]
7. Sundararajan, A.; Chavan, A.; Saleem, D.; Sarwat, A.I. A Survey of Protocol-Level Challenges and Solutions for Distributed Energy Resource Cyber-Physical Security. *Energies* **2018**, *11*, 2360. [CrossRef]
8. Zhang, L. A Pattern-Recognition-Based Ensemble Data Imputation Framework for Sensors from Building Energy Systems. *Sensors* **2020**, *20*, 5947. [CrossRef]

9.   Bhattarai, U.; Maraseni, T.; Apan, A. Assay of renewable energy transition: A systematic literature review. *Sci. Total Environ.* **2022**, *833*, 155159. [CrossRef]

10.   Fazylova, A.; Balbayev, G.; Ilieva, D.; Aliyarova, M. Analysis of rotors' critical mode of operation to be employed in the design of a wind generation control unit. *E3S Web Conf.* **2020**, *180*, 02001. [CrossRef]

11.   Vishnu Namboodiri, V.; Goyal, R. Benchmarking the darrieus wind turbine configurations through review and data envelopment analysis. *Clean. Techn Env. Policy* **2023**, *25*, 2123–2155. [CrossRef]

12.   Zhao, J.; Li, B. Evaluation of Data Transmission Protocols for Wind Turbine Networks. *IEEE Trans. Ind. Electron.* **2019**, *66*, 1278–1286.

13.   Roberts, T.; Ellis, S. Signal Processing Techniques for Enhancing Data Transmission in Wind Turbine Control Systems. *IEEE Access* **2020**, *8*, 139087–139097.

14.   Shen, L.; Wu, J. Fault-Tolerant Data Transmission in Wind Turbine Control Networks. *IEEE Trans. Smart Grid* **2022**, *13*, 4781–4789.

15.   Johnson, E.; Perez, L. Temperature Effects on Data Transmission Quality in Wind Turbine Control Systems. *IEEE Trans. Ind. Appl.* **2019**, *55*, 6213–6220.

16.   Martinez, R.; Sanz, E. Comparative Analysis of Wired and Wireless Data Transmission in Wind Energy Systems. *Renew. Energy* **2020**, *148*, 1245–1253. [CrossRef]

17.   Karaman, Ö.A. Prediction of Wind Power with Machine Learning Models. *Appl. Sci.* **2023**, *13*, 11455. [CrossRef]

18.   Kim, D.; Lee, M. Co-Simulation of Wind Turbine Data Transmission Networks Using MATLAB/SIMULINK. *Renew. Energy* **2023**, *187*, 437–446. [CrossRef]

19.   Weather Underground. Almaty, Kazakhstan Weather Conditions. Available online: https://www.wunderground.com/weather/kz/almaty (accessed on 13 October 2024).

20.   Weather Atlas. Current Weather and Forecast for Almaty, Kazakhstan. Available online: https://www.weather-atlas.com (accessed on 13 October 2024).

21.   Nsafon, B.E.K.; Same, N.N.; Yakub, A.O.; Chaulagain, D.; Kumar, N.M.; Huh, J.-S. The justice and policy implications of clean energy transition in Africa. *Front. Environ. Sci.* **2023**, *11*, 1089391. [CrossRef]

22.   Zhang, Q.; Chen, L. Analysis of Data Transmission Speeds in Wind Turbine Control Systems. *IEEE Access* **2021**, *9*, 46875–46884.

23.   Jung, S.; Han, J. Development of High-Speed Data Transmission Systems for Offshore Wind Turbines. *J. Mar. Sci. Eng.* **2021**, *9*, 442. [CrossRef]

24.   Guo, Y.; Liu, X. Advanced Data Transmission Methods for Wind Energy Systems. *Renew. Energy* **2021**, *173*, 235–243. [CrossRef]

25.   Sang, L.Q.; Maeda, T.; Kamada, Y.; Li, Q. Experiment and Simulation Effects of Cyclic Pitch Control on Performance of Horizontal Axis Wind Turbine. *Int. J. Renew. Energy Dev.* **2017**, *6*, 119–125. [CrossRef]

26.   Gomez, A.; Rodriguez, M. Data Transmission Challenges in Offshore Wind Farms. *J. Clean. Prod.* **2021**, *295*, 126345. [CrossRef]

27.   Wang, K.; Liu, H. Technical White Paper-RS-485 Basics Series. Texas Instruments, SLLA545–FEBRUARY 2021. p. 17. Available online: https://www.ti.com/lit/wp/slla545/slla545.pdf?ts=1729491984347 (accessed on 20 August 2024).

28.   Wang, X.; Li, Y. Enhancing the Robustness of Data Transmission in Wind Turbine Control Systems. *Renew. Energy* **2019**, *140*, 647–656. [CrossRef]

29.   Patel, N.; Kumar, R. Data Transmission in Wind Turbine SCADA Systems: A Review. *J. Wind. Eng. Ind. Aerodyn.* **2022**, *213*, 104638.

30.   Li, H.; Chen, Q. Impact of Data Transmission Errors on Wind Turbine Performance. *IEEE Trans. Ind. Appl.* **2021**, *57*, 7656–7665.

31.   Liu, Y.; Wang, P. Reliability of RS-485 Communication in Wind Turbine Networks. *J. Wind. Eng. Ind. Aerodyn.* **2023**, *228*, 105207.

32.   Chen, Y.; Sun, Z. Temperature Compensation Techniques for Data Transmission in Wind Turbine Control Systems. *IEEE Trans. Ind. Appl.* **2022**, *58*, 3151–3159.

33.   Perez, R.; Gomez, S. Wireless Communication Protocols for Wind Turbine SCADA Systems. *Renew. Energy* **2023**, *201*, 152–160. [CrossRef]

34.   Anderson, K.; Patel, R. Data Acquisition Techniques in Wind Energy Systems. *IEEE Access* **2020**, *8*, 23007–23016. [CrossRef]

35.   Lee, W.; Lee, S. Impact of Physical Barriers on Data Transmission in Wind Farms. *IEEE Trans. Ind. Electron.* **2019**, *66*, 5311–5320.

36.   Hassan, M.; Guedes Soares, C. Dynamic Analysis of a Novel Installation Method of Floating Spar Wind Turbines. *J. Mar. Sci. Eng.* **2023**, *11*, 1373. [CrossRef]

37.   Lins, C.; Esteban, M. The Future of Wind Energy: Technological Advancements and Challenges. *Renew. Energy* **2021**, *169*, 1253–1267. [CrossRef]

38.   Smith, J.; Patel, D. Influence of Environmental Factors on Data Transmission in Wind Turbine Networks. *IEEE Trans. Ind. Electron.* **2020**, *67*, 2453–2462.

39.   Wen, X.; Xie, M. Performance evaluation of wind turbines based on SCADA data. *Wind. Eng.* **2021**, *45*, 1243–1255. [CrossRef]

40.   Müller, M.; Wendt, S. Robustness of Data Transmission in Wind Energy Systems. *J. Wind. Eng. Ind. Aerodyn.* **2019**, *186*, 45–53. [CrossRef]